Supporting information

Two novel Pd thiosemicarbazone complexes as efficient and selective antitumoral drugs

Tania Hidalgo,[a] David Fabra,[b] Raul Allende,[b†] Ana I Matesanz,[b] Patricia Horcajada,*[a] Tarita Biver,*[c] Adoracion G.Quiroga.*[b]

Table of contents

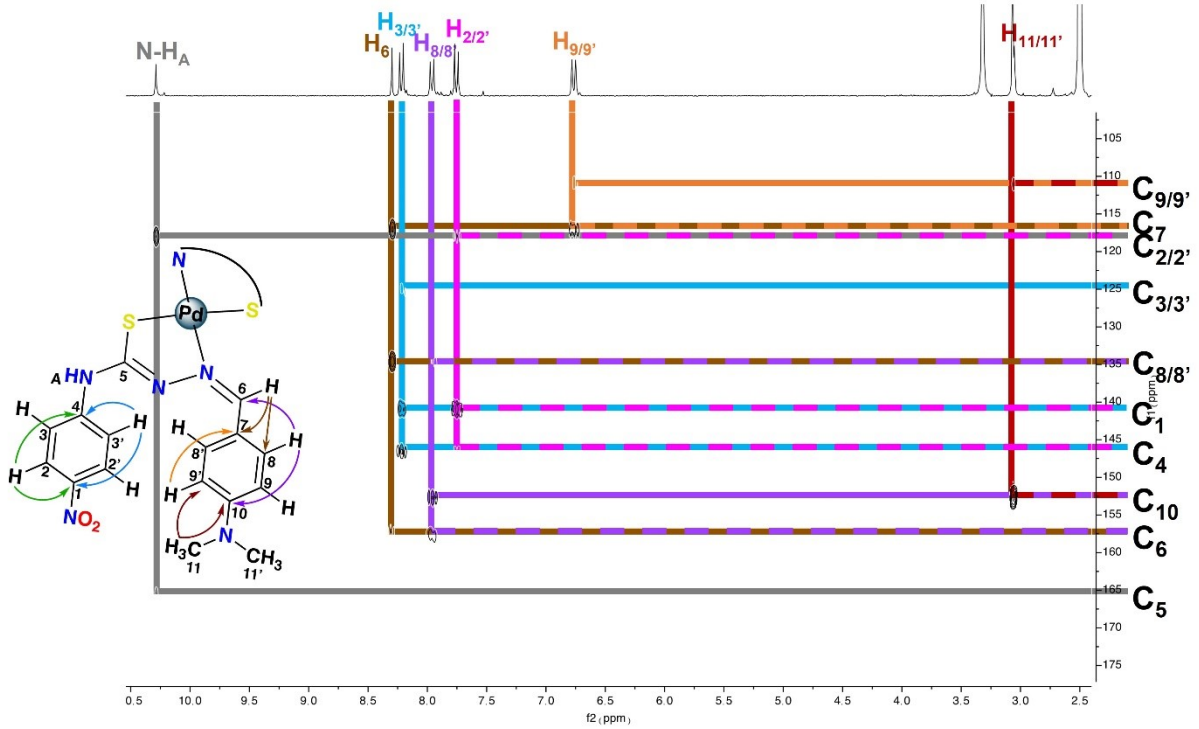

Figure S1. 2D [^{1}H, ^{13}C] HMBC NMR spectra for complex [Pd(L)$_2$].

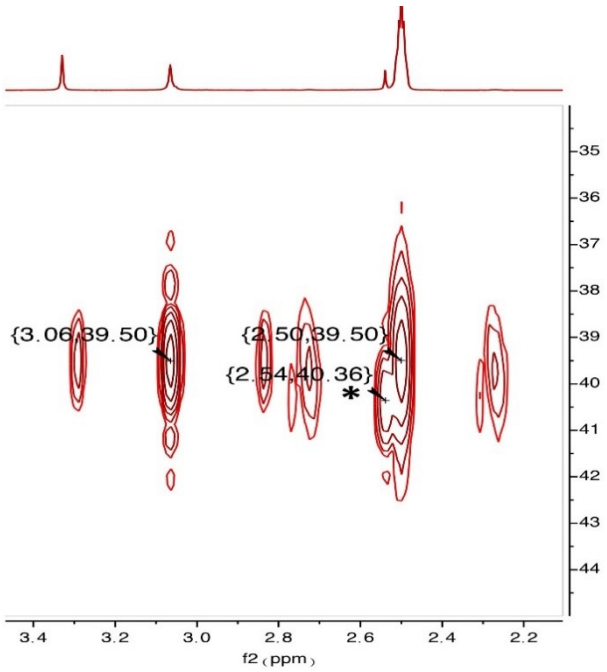

Figure S2. Aliphatic area of the 2D [^{1}H, ^{13}C] HMBC NMR spectra of complex [PdLCl(DMSO)]. The new DMSO methyl group signal is indicated with an asterisk (*).

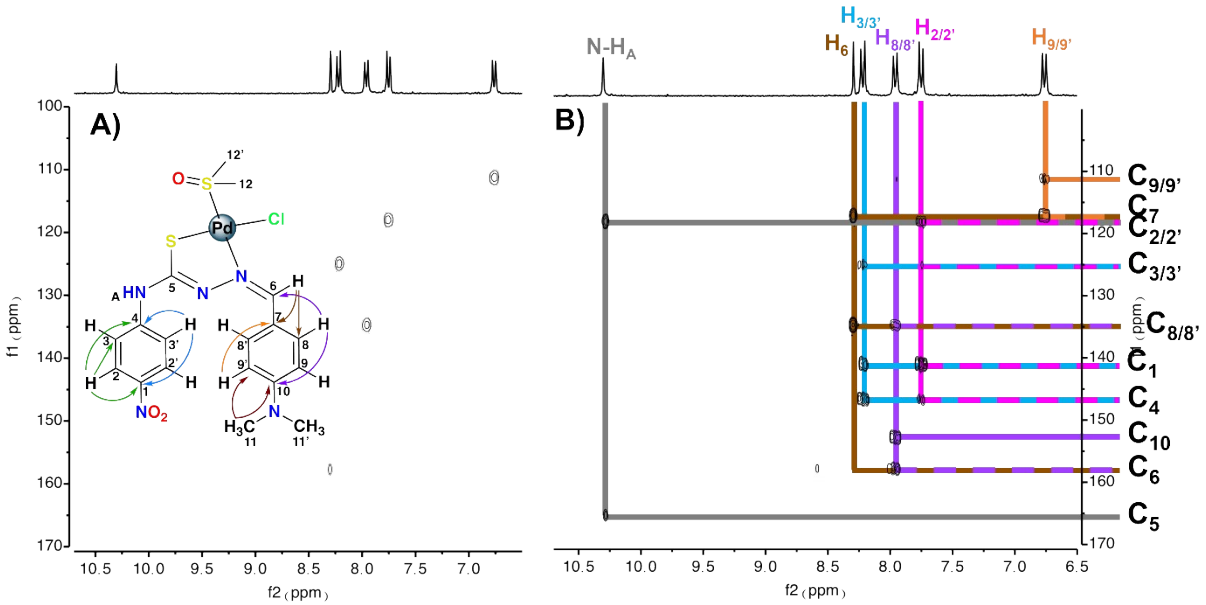

Figure S3. Aromatic area of the spectra (A) HMQC and (B) HMBC for complex [PdLCl(DMSO)].

Table S1. Selected bond distances (Å) and angles (°) for complex [PdLCl(DMSO)].

Bond lengths (Å)		Angles (°)	
C_1–N_2	1.288(9)	N_1–Pd_1–S_1	83.37(19)
C_1–N_3	1.388(10)	N_1–Pd_1–S_2	171.77(19)
C_1–S_1	1.752(7)	N_1–Pd_1–Cl_1	96.67(19)
C_8–N_1	1.297(9)	S_1–Pd_1–Cl_1	177.03(9)
N_1–N_2	1.388(9)	S_2–Pd_1–Cl_1	89.71(8)
Pd_1–Cl_1	2.350(2)	*S_1–Pd_1–S_2	90.53(8)
Pd_1–N_1	2.075(6)	N_6–Pd_2–S_3	84.15(19)
Pd_1–S_1	2.234(2)	N_6–Pd_2–S_4	173.28(18)
Pd_1–S_2	2.249(2)	N_6–Pd_2–Cl_2	96.29(19)
		S_3–Pd_2–Cl_2	179.12(10)
		S_4–Pd_2–Cl_2	89.61(8)
		S_3–Pd_2–S_4	89.99(7)

*As it can be found in the CIF file, the structure shows the presence of two symmetry-independent molecules which do not differ significantly from each other

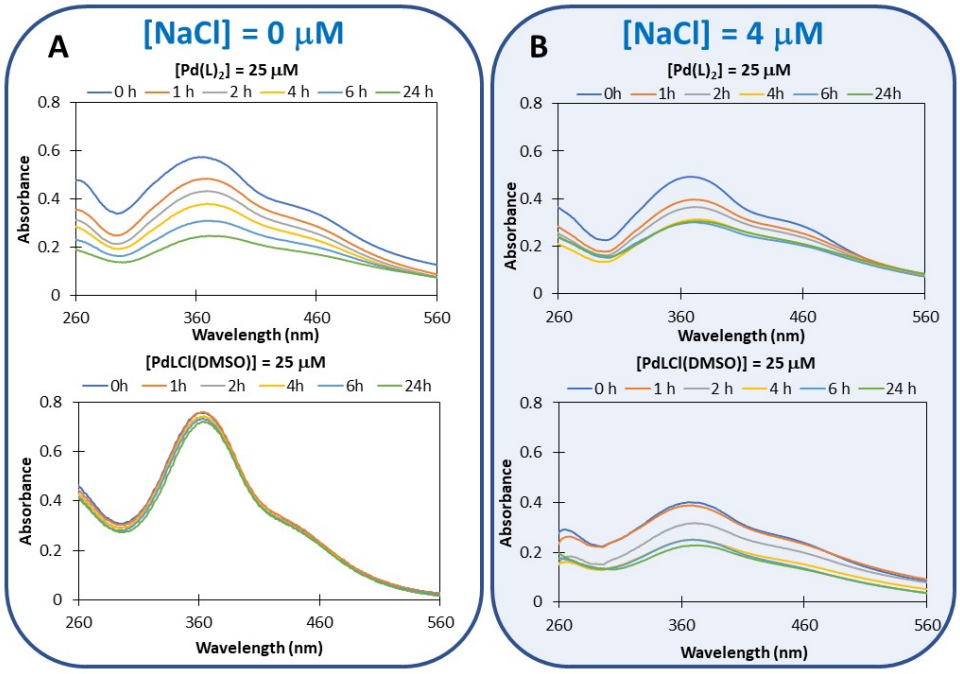

Figure S4. (A) UV-Vis spectra of the complexes $[Pd(L)_2]$ (2.50×10^{-5} M, 3% DMSO) and [PdLCl(DMSO)] (2.50×10^{-5} M, 5% DMSO) in Tris HCl solution, recorded at different times. (B) UV-Vis spectra of the complexes $[Pd(L)_2]$ (2.50×10^{-5} M, 3% DMSO) and [PdLCl(DMSO)] (2.50×10^{-5} M, 5% DMSO) in Tris-HCl solution with 4 µM of NaCl, recorded at different times.

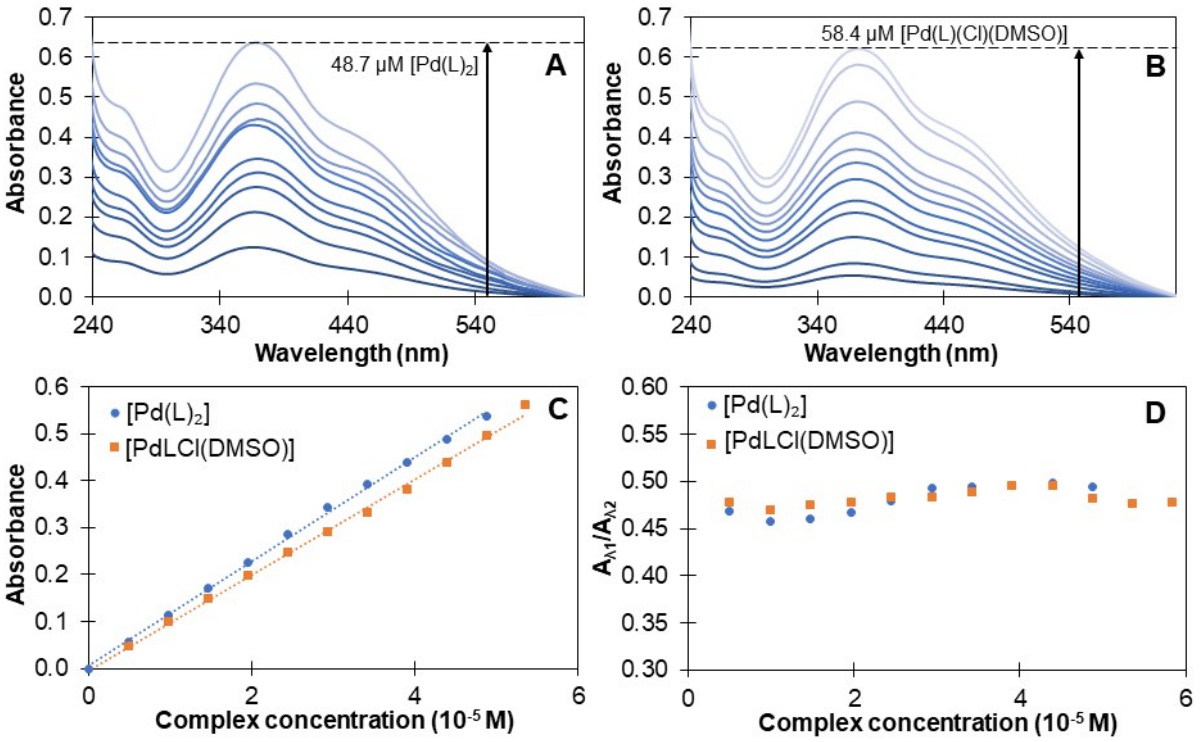

Figure S5. Spectroscopic characterization of $[Pd(L)_2]$ and [PdLCl(DMSO)] complexes in Tris-HCl 5 mM, NaCl 100 mM, pH 7.4 at 25 ºC. (A) $[Pd(L)_2]$ from 4.92×10^{-6} to 4.87×10^{-5} M; (B) [PdLCl(DMSO)] from 4.92×10^{-6} to 5.84×10^{-5} M; (C) Lambert-Beer plots at 371 nm of $[Pd(L)_2]$ ($\varepsilon = 1.11\times10^{4}$ M^{-1} cm^{-1}, blue dot) and [PdLCl(DMSO)] ($\varepsilon = 1.05\times10^{4}$ M^{-1} cm^{-1}, orange square); (D) Absorbance ratio plots of $[Pd(L)_2]$ (A_{299}/A_{371}, blue dot) and [PdLCl(DMSO)] (A_{300}/A_{371}, orange square).

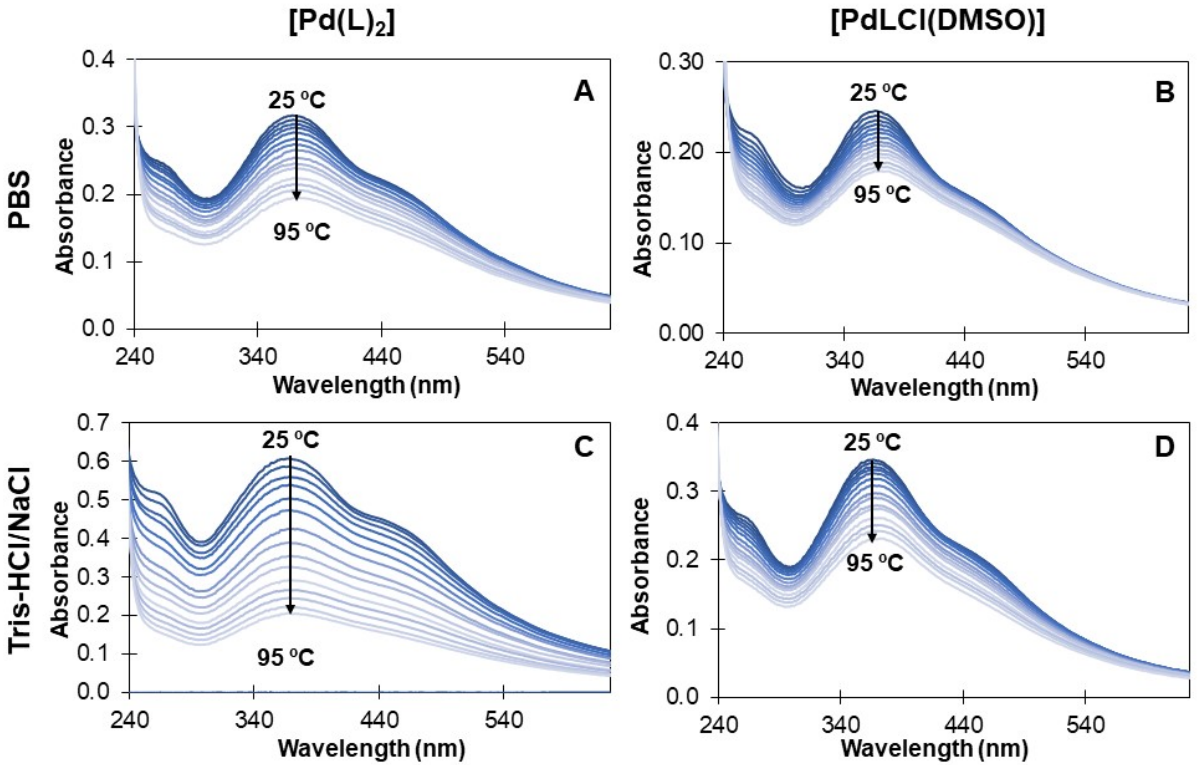

Figure S6. (A), (C) Stability of $[Pd(L)_2]$ as a function of the temperature (from 25 to 95 ºC) in (A) PBS (phosphate 50 mM, NaCl 150 mM, pH 7.2), and (C) Tris-HCl 5 mM/NaCl 100 mM (pH 7.4) buffers; (B), (D) Stability of [PdLCl(DMSO)] with temperature in (B) PBS and (D) Tris-HCl/NaCl buffers (arrows: temperature increase from 25 to 95 ºC). $C_{complex} = 3.57 \times 10^{-5}$ M.

Table S2. IC_{50} and selective index values of $[Pd(L)_2]$, [PdLCl(DMSO)] and cisplatin after 72h of incubation with HL-60, Caco-2 and PC-3 cells.

Complex	IC_{50} (µM)			Selective Index	
	HL-60	Caco-2	PC-3	Caco-2	PC-3
$[Pd(L)_2]$	> 10 (*OOR)	2.10 ± 0.03	1.25 ± 0.13	0.16	0.09
[PdLCl(DMSO)]	> 10 (*OOR)	2.40 ± 0.06	1.22 ± 0.09	0.22	0.11
Cisplatin	0.62 ± 0.05	0.16 ± 0.00	<0.08 (*OOR)	0.26	0.13

*OOR: Out of Range)

Table S3. Effect of [Pd(L)$_2$] and [PdLCl(DMSO)] complexes in the cell cycle distribution of Caco-2 and PC-3 cell line after 72h of treatment. Controls are depicted as negative cells (C-: exposed to no treatment) and cisplatin, as reference compound. Cell cycle checkpoint activation was evaluated by flow cytometry (FACs Melody). Data shown as mean ± S.D of two assays in triplicates.

Cell line	Phase	C-	[Pd(L)$_2$]	[PdLCl(DMSO)]	Cisplatin
PC-3	G0/G1	11.1 ± 2.0	2.2 ± 0.3	13.1 ± 4.2	0.0 ± 0.0
	S	56.3 ± 3.0	94.5 ± 4.0	99.3 ± 1.0	100.0 ± 0.0
	G2/M	37.6 ± 5.5	0.5 ± 0.1	0.1 ± 0.0	0.18 ± 0.1
Caco-2	G0/G1	0.9 ± 0.1	5.4 ± 0.9	6.6 ± 0.5	6.5 ± 1.3
	S	99.0 ± 4.7	89.0 ± 2.3	81.2 ± 6.2	77.0 ± 3.5
	G2/M	2.8 ± 0.3	3.1 ± 0.1	0.1 ± 0.0	0.1 ± 0.0

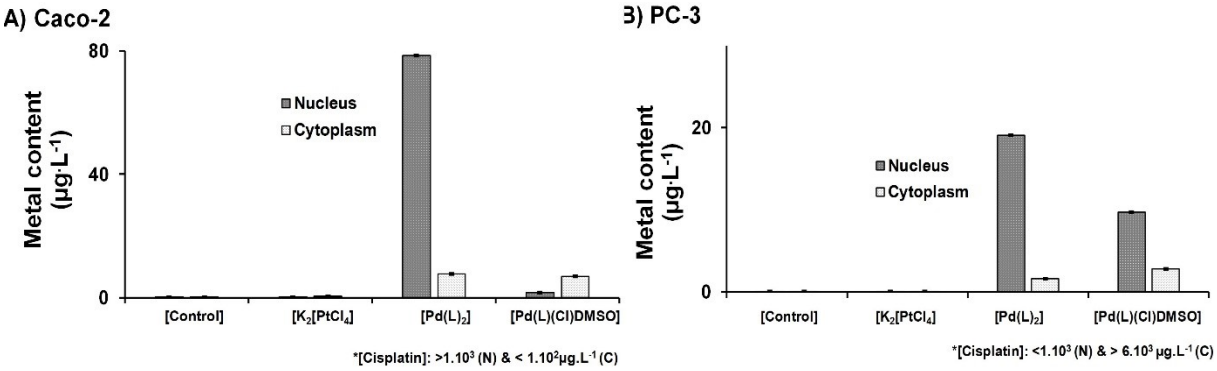

Figure S7. Subcellular distribution of [Pd(L)$_2$], [PdLCl(DMSO)] and their respective precursors in A) Caco-2 and B) PC-3 cells after 72 h of incubation with 5 µM of each complex. Data are expressed as the metal content (µg·L^{-1}) in the nucleus (N) or cytoplasm (C).

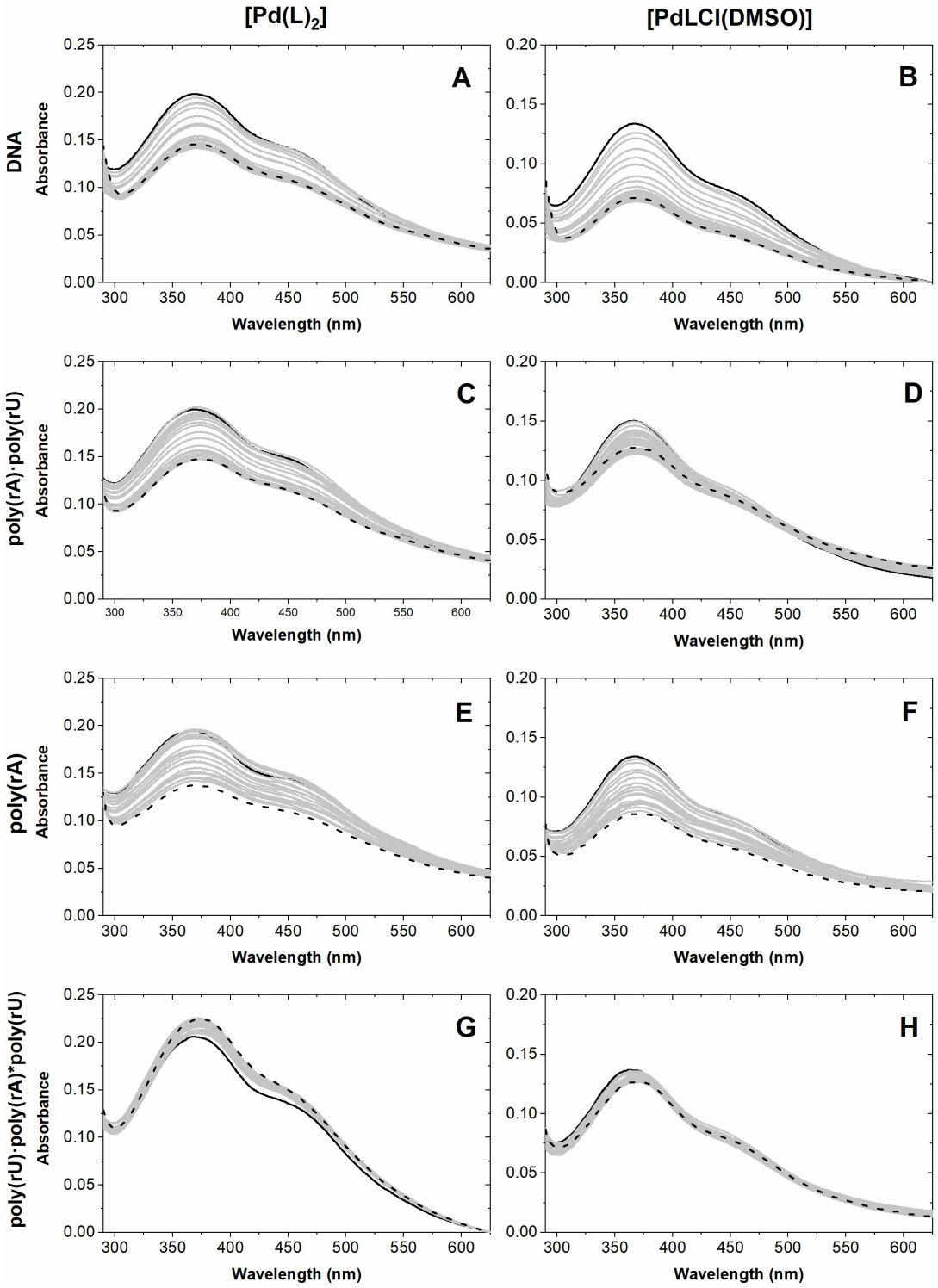

Figure S8. Spectrophotometric titrations of (A) $[Pd(L)_2]$/DNA ($C_{complex}$ = 1.06×10^{-5} M, C_{DNA} from 0 (solid) to 1.67×10^{-5} M (dashed)); (B) [PdLCl(DMSO)]/DNA ($C_{complex}$ = 1.06×10^{-5} M, C_{DNA} from 0 (solid) to 1.69×10^{-5} M (dashed)); (C) $[Pd(L)_2]$/poly(rA)·poly(rU) ($C_{complex}$ = 1.06×10^{-5} M, $C_{poly(rA)\cdot poly(rU)}$ from 0 (solid) to 8.10×10^{-6} M (dashed)); (D) [PdLCl(DMSO)]/poly(rA)·poly(rU) ($C_{complex}$ = 1.06×10^{-5} M, $C_{poly(rA)\cdot poly(rU)}$ from 0 (solid) to 8.10×10^{-6} M (dashed)); (E) $[Pd(L)_2]$/poly(rA) ($C_{complex}$ = 1.06×10^{-5} M, $C_{poly(rA)}$ from 0 (solid) to 3.32×10^{-5} M (dashed)); (F) [PdLCl(DMSO)]/poly(rA) ($C_{complex}$ = 1.06×10^{-5} M, $C_{poly(rA)}$ from 0 (solid) to 2.70×10^{-5} M (dashed)); (G) $[Pd(L)_2]$/poly(rU)·poly(rA)*poly(rU) ($C_{complex}$ = 1.06×10^{-5} M, $C_{poly(rU)\cdot poly(rA)*poly(rU)}$ from 0 (solid) to 5.41×10^{-6} M (dashed)); and (H) [PdLCl(DMSO)]/poly(rU)·poly(rA)*poly(rU) ($C_{complex}$ = 1.06×10^{-5} M, $C_{poly(rU)\cdot poly(rA)*poly(rU)}$ from 0 (solid) to 5.41×10^{-6} M (dashed)); Tris-HCl 5 mM, NaCl 100 mM, pH 7.4, 25 ºC.

Table S4. DNA/BSA binding constants (K_b) values for different Pd(II)-thiosemicarbazone complexes. DNA is always natural DNA from calf thymus. The Log*K* ranges are related to the fact that the reference considers a series of derivatives of the same Pd(II) complex.

DNA BUFFER	pH	T (°C)	DNA conc*	DNA Log K_b	BSA Log K_b	REF/DOI
Tris-HCl (5 mM) NaCl (100 Mm)	7.4	25	bp	6.0 – 6.1	6.5 – 7.2	This work
Tris-HCl (5 mM), NaCl (50 mM)	7.4	37	bp	4.6 – 6.2		10.1016/j.jinorgbio.2019.110875
Tris-HCl (5 mM) NaCl (50 mM)	7.2	RT	P	4.4 – 5.2		10.1016/j.ica.2021.120440
Tris-HCl (5 mM) NaCl (50 Mm)	7.2	RT	P	5.0 – 5.7	4.5 – 6.8	10.1021/acs.inorgchem.0c02373
Tris-HCl (5 mM) NaCl (50 Mm)	7.2	RT	P	4.5 – 5.7	4.1 – 4.5	10.1016/j.molstruc.2020.127703
Tris-HCl (5 mM) NaCl (50 Mm)	7.2	RT	P	4.8 – 6.3		10.1002/aoc.3813
Tris-HCl (5 mM) NaCl (50 mM)	7.2	RT	P	4.8		10.1016/j.jinorgbio.2014.04.017
Tris-HCl (5 mM) NaCl (50 Mm)	7.2	rRT	P	3.8 – 4.4	5.8 – 6.0	10.1021/ic302258k

*DNA conc = way DNA concentration is expressed for K_b calculations, bp meaning in base pairs units while P is phosphates units. The difference between bp and P is supposed to produce no more than 0.3 increase in LogK_b estimation in P.

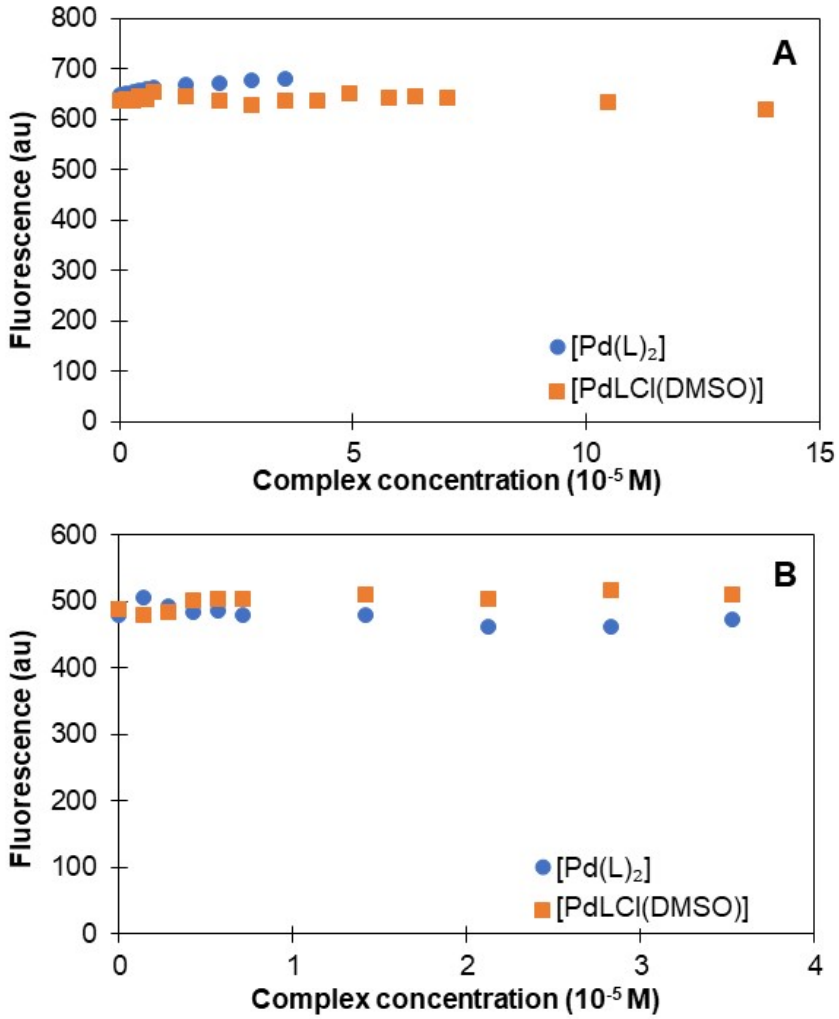

Figure S9. Binding isotherms of fluorescence exchange reaction of (A) EtBr-saturated DNA with $[Pd(L)_2]$ (C_{EtBr} = 9.16×10^{-5} M, C_{DNA} = 2.40×10^{-4} M, $C_{complex}$ from 0 to 3.94×10^{-4} M) and [PdLCl(DMSO)] (C_{EtBr} = 9.16×10^{-5} M, C_{DNA} = 2.40×10^{-4} M, $C_{complex}$ from 0 to 5.68×10^{-4} M), Tris-HCl 5 mM, NaCl 100 mM, pH 7.4, 25 ºC, λ_{exc} = 510 nm, λ_{em} = 595 nm; (B) Et-Br-saturated RNA (poly(rA)·poly(rU)) with $[Pd(L)_2]$ (C_{EtBr} = 7.83×10^{-5} M, C_{RNA} = 2.42×10^{-5} M, $C_{complex}$ from 0 to 3.33×10^{-4} M) and [PdLCl(DMSO)] (C_{EtBr} = 7.83×10^{-5} M, C_{RNA} = 2.42×10^{-5} M, $C_{complex}$ from 0 to 3.32×10^{-4} M) Tris-HCl 5 mM, NaCl 100 mM, pH 7.4, 25 ºC, λ_{exc} = 450 nm, λ_{em} = 585 nm.

Table S5. Crystal data and structure refinement results for compound [PdLCl(DMSO)].

Chemical formula	$C_{18}H_{22}ClN_5O_3PdS_2$
Formula weight (g mol^{-1})	562.37
Temperature (K)	296(2)
Crystal system	monoclinic
Wavelength (Å)	0.71073
Space group	*P*1 21/c1
Crystal size (mm)	0.040 x 0.043 x 0.135
***a* (Å)**	11.2627(6)
***b* (Å)**	26.5445(12)
***c* (Å)**	15.8940(7)
α (°)	90
β (°)	109.7256(14)
γ (°)	90
Volume (Å^3)	4472.9(4)
Z	8
Density, calculated (g cm^{-3})	1.670
Absorption coefficient (mm^{-1})	1.166
F(000)	2272
θ range for data collection (°)	1.53 – 25.35
Reflections collected	70909
Independent reflections	8190 [R(int) = 0.1394]
Coverage of independent collections (%)	100.0
Data/restrains/parameters	8190 / 0 / 549
Goodness of fit on F^2	1.035
Final R indices [*I>2σ(I)*] / all data	R1 = 0.0499 / 0.1260 wR2 = 0.1084 / 0.1643
Largest diff. peak and hole, (e Å^{-3})	0.705 and -0.848